Journal of Magnetism and Magnetic Materials 322 (2010) 3035–3040

Contents lists available at ScienceDirect

Journal of Magnetism and Magnetic Materials

journal homepage: www.elsevier.com/locate/jmmm

Effects of substitution of Mo for Nb on less-common properties of Finemet alloys

P. Butvin [a,*], B. Butvinová [a], J.M. Silveyra [b], M. Chromčíková [c], D. Janičkovič [a], J. Sitek [d], P. Švec [a], G. Vlasák [a]

[a] Institute of Physics, Slovak Academy of Sciences, Dubravska cesta 9, 845 11 Bratislava, Slovak Republic
[b] Instituto de Technologías y Ciencias de la Ingeniería H.F. Long, Facultad de Ingeniería, UBA-CONICET, Buenos Aires, Argentina
[c] Vitrum Laugaricio – Joint Glass Centre of the Inst. of Inorg. Chem., SAS Bratislava and A. Dubček University of Trenčín, 911 50 Trenčín, Slovak Republic
[d] Dept. of Nuclear Phys. & Technol., FEI, Slovak University of Technology, 812 19 Bratislava, Slovak Republic

ARTICLE INFO

Article history:
Received 17 December 2009
Received in revised form
22 March 2010
Available online 19 May 2010

Keywords:
Dilatometry
Magnetic anisotropy
Magnetic measurement
Mössbauer spectroscopy
Nanostructured material
Thermomechanical processing

ABSTRACT

Particular properties of Fe–Nb/Mo–Cu–B–Si rapidly quenched ribbons were examined. Apart from minor variation, no significant difference due to the Mo for Nb substitution was observed in alloy density and its annealing-induced changes. The same holds for the anisotropic thermal expansion of as-cast ribbon when annealed and for induced anisotropy when annealed under stress. The Mo-substituted ribbons show only slightly higher crystallinity and lower coercivity if annealed in inert gas ambience than in vacuum. Some diversity in surface to interior heterogeneity of the differently annealed ribbons can still be distinguished. Preserving a minor percentage of Nb together with Mo does not seem substantiated to obtain favorable soft magnetic properties of ribbons annealed in inert gas.

1. Introduction

The idea to try other refractory metals instead of Nb came soon after the introduction of Finemets with incipient understanding of the role of Nb [1]. So Ta, W, Mo and Zr, Cr and V were used to substitute a part or all of Nb in the basic Fe–Nb–Cu–B–Si composition. The first attempts aimed at preserving and/or improving the good soft-magnetic properties of Finemet. The substituting elements sorted as for the best results appear mostly: Nb ≥ Ta > Mo ≥ W > V > Cr. The magnetic properties were represented by relative permeability at 1 kHz measured on toroidal samples annealed at 550 °C in nitrogen [1]. Although the grain size decreased further, by increasing the percentage of Nb or its substitutes over 3 at%, the magnetic properties got worse. Many of recent work appear to show that some Nb (∼1 at%) should be retained at the substitution to achieve the best magnetic properties which are seen as principally due to non-agglomerated, as fine as possible Fe–Si grains [2]. With the partial substitution, annealing in hydrogen and considering additional magnetic parameters (coercivity, core loss), the order of successful substitutes Ta > W > Mo was only slightly different. Further research showed that unlike Nanoperms and Hitperms, in Finemets both Cu and Nb are necessary to provide for the optimal nanocrystalline structure through pre-nucleation clustering and grain growth hindering, respectively [3]. Whereas authors reporting on higher Mo, Si-free alloys (5–8 at% Mo) consider partial incorporation of Mo into bcc-Fe grains [4], low Mo alloys do not reveal any signs of Mo within the grains. This appears to hold equally for alloys with tiny contents of Nb [5] as well as for Si-containing alloys where Si shrinks the Fe–Si lattice and so could obscure a XRD identification of any small Mo share within the grains [6].

It remains unclear what is the role of tiny amount of Nb which appear to provide the better soft-magnetic properties if compared to alloys with all of Nb substituted by Mo. Although diverse annealing environment was used in the works cited above (Ar, H_2, N_2, vacuum), we found no single work where samples annealed in vacuum and gaseous environment were compared to see whether possible surface effects could be significant for the Mo for Nb substituted alloys. Similarly, no systematic data concerning the alloys density and its changes due to thermal treatment are available so far. Changing density can pose a risk of generating internal stresses. We also found no check of the response to stress annealing in the literature. The use of the better available and cheaper Mo instead of Nb is particularly appealing for practical use [7]. Therefore, we chose to examine the four above-mentioned unclear points concerning the Fe–Nb/Mo–Cu–B–Si alloy system.

* Corresponding author: Tel.: +421 2 59410560; fax: +421 2 54776085.
E-mail address: pavol.butvin@savba.sk (P. Butvin).

0304-8853/$ - see front matter © 2010 Elsevier B.V. All rights reserved.
doi:10.1016/j.jmmm.2010.05.025

2. Materials and methods

The amorphous precursor ribbons were prepared by planar-flow casting of the melt in air. All the ribbons were 10 mm wide; the average thickness was 19 μm. Particular composition is quoted in Table 1. Standard methods were used to test the composition, structure, grain size (by TEM) and to perform Mössbauer spectroscopy (MS). The popular Normos software has been exploited to evaluate MS. In-house developed technology was used to determine the density and magnetostriction by buoyancy (Archimedean) method and a capacitive-sensor-based apparatus, respectively. Despite of small sample volume, the density is determined with an accuracy of $\pm 0.5\%$. Thermal expansion and its as-cast anisotropy have been checked using a commercial dilatometer. Rectangular strip samples were submitted to all the measurements. Magnetic measurements (loop recording) were performed on toroids too. The toroidal cores showed 30/34 mm inner/outer diameter in average and masses 7.7–8.9 g. Samples were excited by 21 Hz signal from a low output impedance amplifier. The difference between the input impedance of Helmholtz coils primary (where the strip was inserted) and the toroid primary caused significantly lower harmonic contents in toroid response signal—toroids worked almost in sinusoidal induction regime if not oversaturated. This systematic difference is reflected for instance in Fig. 3. Whereas the cross section of a strip was below 0.2 mm^2, a toroid attained 12 mm^2 in average. The true cross section used to compute the magnetic polarization J and induction B (strips and toroids, respectively) was not directly measured but computed using density, mass, ribbon width and other dimensions (length for strips, outer and inner diameter for toroids). The loops recorded for strips are corrected for demagnetization by plotting the polarization J against the internal field H_i computed as $H_i = H_{ext} - DJ/\mu_0$, where the demagnetization factor D was evaluated from the strip dimensions using elliptic integral calculation. To address the changes of magnetic anisotropy, the quantity W (J/m^3) inferred from the so-called magnetization work [8] was computed from the digitized loops according to

$$W = -\int_{J_s}^{J_r} H_i \, dJ \quad (1)$$

where J_s and J_r is the maximum attained polarization and remanent magnetic polarization, respectively. Thermal treatment of samples has been performed in inert gas (Ar) atmosphere without prior evacuation of the furnace, reference samples were annealed in vacuum ($p < 10^{-3}$ Pa).

3. Results and discussion

The alloys show thermal and structural properties as known from earlier works [1,9]. The onset temperature of the first crystallization stage ranges from 490 to 520 °C—the less Mo the higher the temperature. The second crystallization stage, which enables crystalline borides to appear, sets on safely above 600 °C for all the studied compositions [10]. After 550 °C 1 h annealing, the crystalline grain dimensions do not surpass 15 nm in any alloy. The average bcc Fe–Si (with DO3 superstructure) grain dimension is ~10 nm as already reported [9,11]. Unlike Si-free Fe–Mo–Cu–B ribbons, where peculiar occurrence of surface crystals was detected [12], no similar surface anomalies were observed on the studied Fe–Mo–Cu–B–Si ribbons. Matching the earlier results [1], the increasing Mo to Nb ratio is seen to decrease negligibly the Curie temperature T_C of the as-cast alloys down to ~320 °C [10].

3.1. As-cast properties

The as-cast ribbons (as well as toroids wound of it) show typical round hysteresis loops which do not saturate even at 2 kA/m exciting field. There is no discernible systematic correlation to the composition. Nevertheless, Mo3 shows the least magnetic anisotropy just about saturating at 1.18 T, simultaneously displaying the lowest as-cast dynamic coercivity H_{cd} of ~10 A/m. The magnetostriction shows values (see Table 1) typical for similar materials. The density of all the alloys (see Table 1) is confined within a range hardly surpassing the accuracy ($\pm 0.5\%$) of the method used. Apart from the former insignificant differences, it appears that the coexistence of Mo with Nb results in a slightly lower density if compared to Mo-only or Nb-only compositions.

3.2. Annealing effects

The density definitely increases due to annealing as generally observed for Si-rich (more than 12 at% of Si) Fe-based ribbons. The annealing at a temperature between the first and the second crystallization stages causes a density increase of about 2% in contrast to Si-poor Finemets [13], similar Si-free compositions (e.g. Fe–Mo–Cu–B) or Hitperms [14], where the increase is often below 0.5%. Whereas the change of density represents the true volume change, linear dilatation is not generally reliable as to the volume changes, but provides other instructive information. The as-cast ribbons show anisotropic behavior when linear dilatation is measured along and transverse to the ribbon axis—Fig. 1.

The effect was observed on metallic glasses years ago [15] but found little attention. Unlike the longitudinal dilatation showing reduced expansion (frequently referred to as structural relaxation [16]), a process resembling viscous flow or creep appears to be effective during transversal dilatation between 200 and 450 °C. Stress annealing serves the hint to creep. Longitudinal dilatation under 33 MPa tension shows both the reduced expansion and creep, where the creep only takes over above 360 °C until the crystallization shrinkage prevails at ~515 °C. The orthogonal

Table 1
Alloy composition and properties.

Composition (at%)	Label	ρ (g/cm^3)		$\lambda_s \times 10^6$		J_s (T)
		As-cast	Anneal vacuum	As-cast	Anneal vacuum	Anneal vacuum
$Fe_{73.5}Nb_3Cu_1B_9Si_{13.5}$	Mo0	7.28	7.39	18.5	2.0	1.22
$Fe_{73.5}Mo_{1.5}Nb_{1.5}Cu_1B_9Si_{13.5}$	Mo1.5	7.18	7.34	26	1.8	1.21
$Fe_{73.5}Mo_2Nb_1Cu_1B_9Si_{13.5}$	Mo2	7.23	7.36	16	2.6	1.21
$Fe_{73.5}Mo_3Cu_{0.8}B_{9.1}Si_{13.6}$	Mo3	7.26	7.40	18	1.8	1.24

Density ρ, coefficient of saturation magnetostriction λ_s for as-cast and 540 °C/1 h annealed alloys. Room-temperature saturation magnetic polarization J_s (at $H = 150$ A/m) is quoted in the rightmost column.

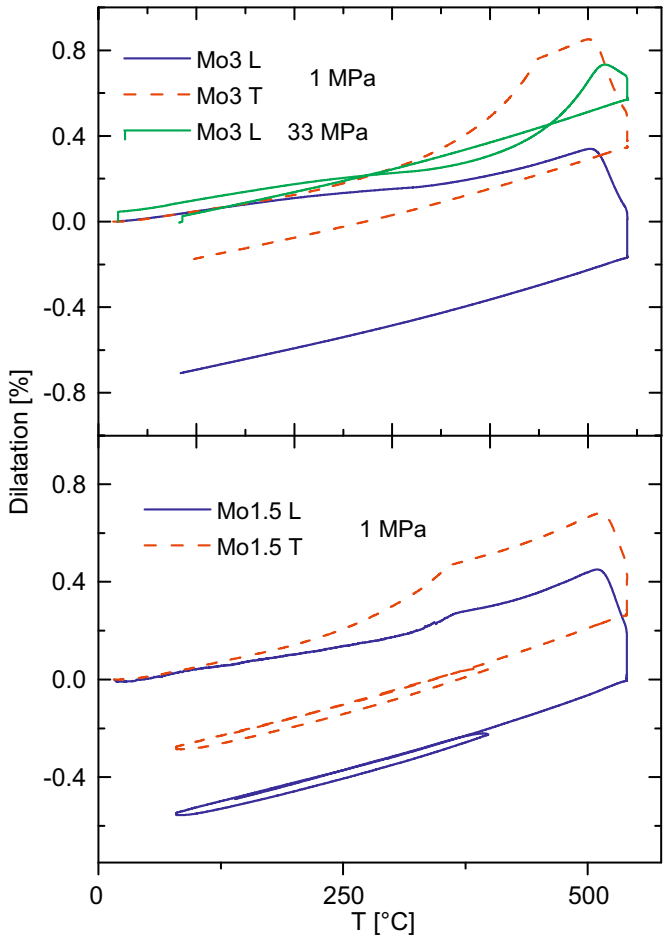

Fig. 1. Linear dilatation (dimension change to dimension at 20 °C) measured along (L) and transverse (T) to ribbon axis for indicated samples at 10 K/min temperature rate. Samples were held at 540 °C for 40 min. MPa values identify tensile stress applied along measurement direction.

measurements under the low 1 MPa stress compared to each other show the complete result of the anisotropic behavior: The ribbon shrinks longitudinally far more than transversally and this is not due to the crystallization shrinkage, which in both directions attains approximately 0.55% and 0.42% of the as-cast dimension of Mo3 and Mo1.5 samples, respectively. Although, this isotropy observed at crystallization of Mo Finemets is not a general principle since we observed the crystallization shrinkage to be clearly anisotropic in many similar ribbons [17]. Thus, if we subtract the isotropic crystallization shrinkage from the final dimension change, we see that the amorphous ribbon expanded transversally and shrunk longitudinally. The coefficient of thermal expansion (CTE) determined at 1 MPa loses much of its anisotropy right above the apparent "critical" temperature (the sudden drop of CTE at 450 °C for Mo3T—see Fig. 1) and becomes all but isotropic showing the value of $\sim 11\mathrm{E}-6\,\mathrm{K}^{-1}$ after the partial nanocrystallization. The anisotropic thermal expansion is thus annealed out. This was confirmed by submitting the nanocrystallized ribbons to another temperature cycle from room temperature to 400 °C and back. Unlike Mo3, Mo 1.5 shows the sudden drop of CTE on longitudinal expansion too. The corresponding apparent critical temperature (360 °C) is lower than for Mo3 and again it is stress sensitive. The CTE drop is rarely observed on similar materials and if so, it is not that sudden.

There are principally two strains which can show anisotropic relaxation at increasing temperature—the anelastic strain due to an anisotropic casting stress and the magnetostrictive strain. Up to T_C, the sample of a positively magnetostrictive material is "pre-elongated" (most along the resulting averaged magnetization) and correspondingly "pre-shrunk" along a perpendicular direction. Nevertheless, the magnetostrictive strain is two orders less ($\lambda_s \sim 0.002\%$—Table 1) than for instance the transversal elongation observed up to the CTE drop at 450 °C for Mo3T (Fig. 1) and this apparent critical temperature is very stress-sensitive and too high to correspond to the amorphous Curie temperature ($T_C \sim 320$ °C according to DSC [10]). The 1 MPa measuring stress is enough to promote discernible viscous flow in some Hitperms [14] but not in Finemets [18]. Moreover, the creep induced by 33 MPa sets on at no lower temperature than 360 °C, whereas the seemingly similar transversal elongation supported by mere 1 MPa starts at significantly lower temperature. Therefore, the apparent similarity is insufficient to regard the elongation at 1 MPa as creep or viscous flow. Most probably, this effect of creep-like elongation is due to the relaxation (recovery) of the anisotropic as-cast residual strain. The apparent critical temperature then marks the termination of the as-cast anisotropy relaxation. Apart from the stress sensitivity, this temperature is seen for any composition to vary modestly from ribbon to ribbon, so looking for a correlation to the composition within this work has not been found reasonable. Still another vulnerable factor at dilatometry is the strain introduced by cutting the anisotropic rough-surface samples. To minimize the influence of probable cutting-strain recovery, samples as large as possible were subjected to dilatometry. Equal shape and equal size samples were always used for the longitudinal-transversal comparisons. The annealing behavior as seen by dilatometry is an important factor to be considered particularly when more massive compact components (a ribbon-wound toroid) are intended for annealing.

3.2.1. Stress annealing

If longitudinal dilatation at 1 and 33 MPa stress is compared to each other, the 33 MPa stress appears to increase the crystallization-onset temperature by ~15 K (Fig. 1). This temperature shift might account for some deficit in crystalline share in stress-annealed samples if compared to no-stress equivalently annealed ones. Whereas two papers report such a deficit [19,20], we found also a contradictory interpretation of measurements [21] on similar materials.

The stress-annealing-induced magnetic anisotropy is of the hard-ribbon-axis (HRA) type. The modest tensile stress of 33 MPa is quite enough to induce a significant HRA anisotropy characterized by W of almost 400 J/m^3 which is fully comparable to Nb Finemets. The corresponding loop is compared to two references in Fig. 2. The 15.5 at% Si Finemet (Nb3Si15.5) has been chosen as the reference because it shows the largest stress-anneal-induced anisotropy from among the Nb Finemets and the ribbon thickness equals that of Mo3 enabling the use of equal demagnetization factor and to attain equal stress with the use of equal force. Whereas the slim loops displaying large HRA anisotropy (i.e. $J_r \to 0$, see relation (1)) are optimal for exploiting the conditional equivalence of magnetization work and anisotropy [8], the different saturation represents an impediment to straightforward comparison. Thus, we scaled the Nb3Si15.5 loop preserving its genuine slope so as to attain the Mo3 saturation. Then the reference value for Nb3Si15.5 is $W \sim 475$ J/m^3. The stress-annealed sample Mo3 does not saturate well so the above-mentioned modest crystallinity deficit could not be reliably identified by a corresponding saturation deficit.

3.2.2. Soft magnetic properties

Apart from the consequences of stress annealing, the conventionally annealed (1 h isotherm) samples show the room

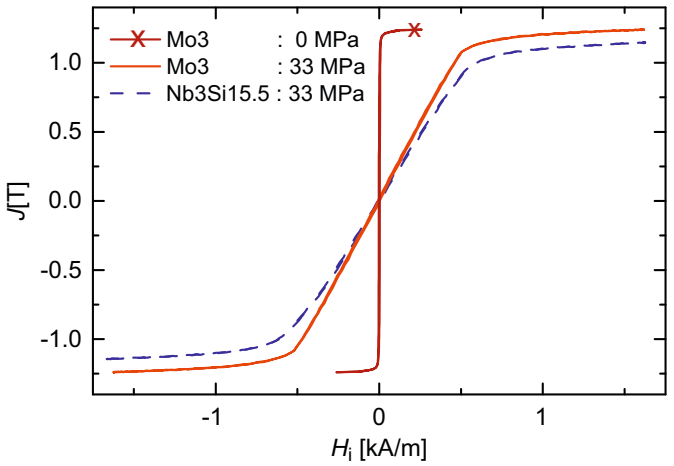

Fig. 2. Loops of strips annealed (540 °C/1 h) in Ar under the tensile stress as indicated after colon.

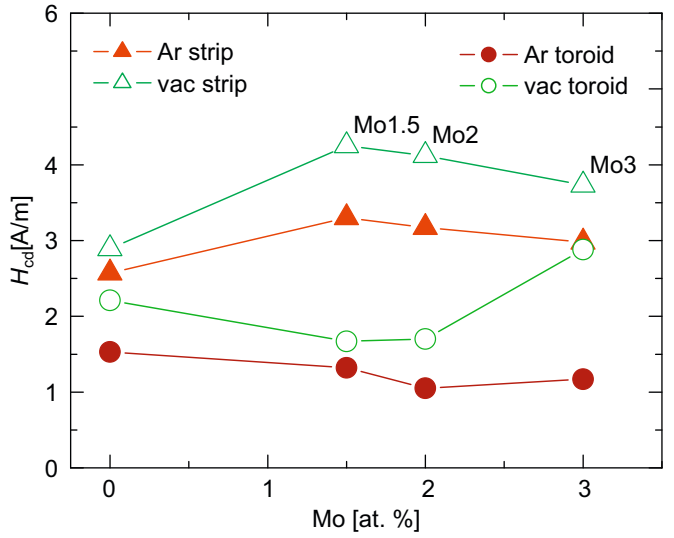

Fig. 3. Variation of dynamic coercivity for indicated composition and sample type after 540 °C/1 h annealing in indicated ambience. Value of the "best" core is plotted for Mo3 vacuum annealed toroid—consult Fig. 5.

temperature saturation to increase by some 6% due to the standard 540 °C annealing if compared to the as-cast state. The magnetostriction is substantially reduced (Table 1) and the coercivity H_{cd} decreases down to 1 A/m—Fig. 3. Nevertheless, effect of a higher annealing temperature was tested as well. Increasing the temperature to 570 °C has not been found to bring any additional risks with any of the Mo Finemet ribbons. In contrary, an improved but hardly significant decrease of H_{cd} and increase of J_s has been observed after 570 °C—1 hour vacuum annealing.

3.2.3. *Influence of annealing ambience*

The differences observed between vacuum annealed and gas annealed sample properties are small if compared to, for instance, Si-poor Nb Finemets [22]. Even the small differences still appear to correlate to different annealing ambience as seen in Fig. 3 and Table 2. Unlike the strip–toroid difference that is explained in part 2, the larger H_{cd} values for vacuum annealed samples show another diversity that appears to be due to the annealing ambience. Mössbauer spectra were evaluated on the assumption that the Fe-based crystalline phase is well characterized by the

Table 2
Mössbauer spectroscopy parameters.

Alloy	$\langle H \rangle$ (T)		A_{23}		A_{cr} (%)	
	Vacuum	Ar	Vacuum	Ar	Vacuum	Ar
Mo0	19.1	18.5	3.30	3.31	51	52
Mo1.5	20.5	18.7	2.25	2.99	33	57
Mo3	20.0	19.5	3.14	3.98	35	55

The samples were annealed at 540 °C for 1 h in indicated ambience. Hyperfine field $\langle H \rangle$ and A_{23} ratio (see text) refer to the amorphous rest. A_{cr} is the crystalline share determined from particular spectrum area.

DO3 superlattice. Thus, the term "crystallinity" is to be understood in a somewhat narrower sense in this paragraph. Whilst Ar annealing of the Mo Finemets results in a crystallinity which matches well that of the corresponding Nb Finemet, the vacuum annealed Mo Finemets show slightly less crystalline share and larger hyperfine field $\langle H \rangle$. Another MS parameter, which shows an Ar—vacuum difference, is the ratio A_{23}. It gives information about the orientation of the ^{57}Fe magnetic moment within the amorphous rest: value of 4 means the moment lies in plane, whereas 0 stands for normal to plane of the ribbon. Ar annealed samples show more magnetic moments to lie in the ribbon plane than the vacuum annealed samples do. Thus, a corresponding different magnetic anisotropy could be expected. Indeed, comparable loops recorded for strips as well as for toroids show W – relation (1) – larger for vacuum annealed samples than for Ar annealed ones by approximately 25%. The values of W ranged from 1.5 to 4.5 J/m^3, thus the off-axis anisotropy is weak. Nevertheless, the coincidence of smaller A_{23} and larger W for vacuum-annealed samples can be seen as a sign of minor off-plane anisotropy, which is suppressed in Ar-annealed samples.

An off-plane anisotropy where the easy axis is not contained in the ribbon plane is quite common in soft-magnetic ribbons prepared by planar-flow casting. It comes from surfaces that exert an in-plane stress on the magnetostrictive ribbon interior and produces a characteristic magnetoelastic contribution to the anisotropy. We use the term macroscopic heterogeneity (MH) [22] to name the principal cause of the above effect. The heterogeneity can often be identified as surface-to-interior compositional difference by XPS and/or SIMS. It comes right with as-cast ribbons and changes itself [23] as well as its influence due to thermal treatment. In Si-poor compositions, the MH appears to promote surface crystallization [24] but this is by far not the only effect, which can create the in-plane stress. Whereas magnetic response to MH is quite significant for strongly magnetostrictive materials as Hitperms [14], MH can cause very weak effect, particularly for the Finemets containing 13–14 at% of Si. It is worth noting that this is not the composition with the least magnetostriction. With the assumption that MH acts in Mo Finemets through surfaces feebly pulling (spreading) the ribbon interior, we can offer the explanation why Ar-annealed samples show weaker HRA anisotropy: Spreading the positively magnetostrictive ribbon pushes the value of A_{23} to 4 (Table 2) and diminishes W by aligning the easy direction to the ribbon plane in the major part of the ribbon (interior). To test this hypothesis, we etched out the Ar-annealed strip-samples' surfaces of two diversely thick Mo3 ribbons. The surface removal resulted in ~1 μm thickness reduction for both the ribbons. The loops (two not-adjacent samples of each ribbon were equally etched) got a slight tilt as seen in Fig. 4 and attained larger W akin to vacuum annealed samples, which show a value around 4 J/m^3.

The tilt acquired by etching (i.e. ΔW) was larger for the thicker ribbon. Etching is not limited to merely remove the surface but it can simultaneously create a new—altered one and this could

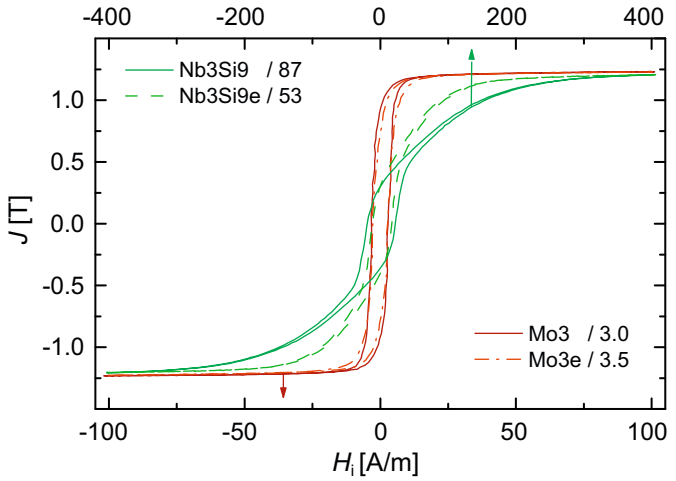

Fig. 4. Loops of Ar annealed (540 °C/1 h) strips before and after surface removal by etching. "e" before slash denotes the latter. The number after slash indicates magnetization work W (J/m^3). Note that the upper H scale refers to Nb3Si9 loops (see text for full composition).

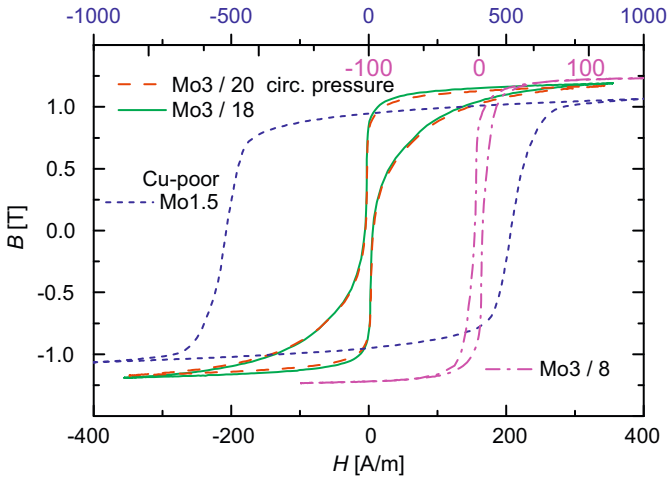

Fig. 5. Loops of vacuum (540 °C/1 h) annealed toroids. The number after slash indicates magnetization work W (J/m^3). The "best" vacuum annealed Mo3 core shows the loop which is together with its upper H scale right-shifted at plotting—the corresponding H scale is upper right. The loop of similar but Cu-poor alloy with precipitated borides after the same annealing is plotted for comparison—its H scale is on the top axis.

apply different stress of its own. If the altered surfaces would exert an equal squeeze, larger ΔW should be expected for the thinner ribbon however, the opposite was observed. Reference etching experiment with a Si-poor Finemet ($Fe_{75}Nb_3Cu_1B_{12}Si_9$), which features squeezing (compressing) surfaces [25] and a slant loop after Ar annealing, showed opposite response. The surface removal resulted in 2.4 μm reduction of thickness (11%) and 40% decrease of W clearly diminishing the loop tilt. Surface morphology (roughness) cannot explain the observed results. Checking the surfaces by microscope did not reveal any discernible diversity of morphology between genuine and etched samples. Accordingly, no opposite changes of surface texture due to etching were detected on the samples showing the opposite changes of W. Thus we regard the etching experiment with Ar annealed Si-rich Finemets as showing the effect of spreading surfaces removal. Nevertheless, the influence of MH is exceptionally small for the Si-rich Mo Finemets as well as for similar Nb Finemets.

3.2.4. *Peculiar loops*

Unlike the widely held opinion [2,6], that the best soft-magnetic properties are obtained if not all Nb is substituted by Mo, our results point to the fully Mo-substituted alloy showing the best parameters (B_s/H_{cd}). However, there probably is a critical exception. While all the alloys of the Fe–Mo–Cu–B–Si series show standard low-anisotropy low-loss loops, the Mo3 vacuum-annealed toroids provided a not well reproducible peculiarity—displayed in Fig.5. Keeping all the known parameters (core construction, annealing conditions) as equal as possible, we tested one toroid after another whether the constricted loop shows up systematically.

On the fourth trial, we finally observed a significantly less constricted loop. Longitudinal ribbon inhomogeneity is hardly the reason since none of the ribbon pieces cut between the core-bound segments as well as none of the Ar-annealed toroidal cores displayed similar constricted character of its loop. Apart from a slight Cu deficit – the analysis shows 0.8 at% of Cu – there is nothing suspect on the composition. There is no large grain, no clumped grains, and no borides as one would probably expect from slightly less Cu. By chance, there was a Cu-poor (0.4 at% only) Mo Finemet in our archive and we tested it—its loop is also displayed scaled in Fig. 5. Borides have been identified after the annealing. The resulting coercivity increase resembles the one observed in Ref. [9] at temperatures close to the second crystallization on alloys with "correct" composition. This is for sure not the reason for the peculiar loop because the reference loop shows quite another character and the coercivity of Mo3 strips do not increase even after 570 °C annealing. The most probable reason for the constricted loop is a not well reproducible stress within the core. Minor circumferential compression was exerted on the annealed core by a rubber ring ("tight belt") and the loop shows still more difficult magnetization (1st and 3rd quadrant) than the genuine constricted loop. There are reasons to think of non-negligible internal stress in the Mo3 cores: Whereas the cores of the other compositions show packing factors 0.74–0.80, the Mo3 cores are the densest with a packing factor over 0.86, despite different Mo3 ribbons showing the effective thickness of 22 and 18 μm were used to wind the cores. This appears to correlate with qualitative microscopic observation of the surfaces—Mo3 ribbons show the smoothest surface of the whole series. Other materials show better the well-known tendency of ribbon-wound cores—the thinner the ribbon the lesser the packing factor. A ribbon-wound core of ~9 g mass can hardly heat up homogeneously at a rate of ~10 K/min (the rate at 500 °C where the ribbon begins to shrink—Fig. 1). If a force coming from inhomogeneous core shrinkage during annealing is to be relaxed by relative movement of adjacent turns, the ensuing friction energy can be larger as in more loosely packed cores and possibly induces a shear stress. Such a stress could influence the core as a residual stress or even during annealing. In this context, we recall the possibility to induce a significant stress-induced anisotropy in this material (Fig. 2). Nevertheless it remains unclear where an unintended stress showing the above "tight belt" effect comes from, just and only at the vacuum annealing. On the other hand, such a loop is rather rare and interesting also as to the underlying magnetization process, so further devoted work is in progress. Thus, the Mo3 alloy could be considered as promising but potentially risky for the time being.

4. Conclusions

In general, the substitution of Mo for Nb in the standard Finemet composition brings no notable difference to structural characteristics and no clear risk or detriment to the desired soft

magnetic properties. The particular questions, which motivated this work, are answered as follows:

- The annealing of Fe–Mo/Nb–Cu–B–Si ribbons in inert gas ambience brings slightly better soft magnetic parameters than vacuum annealing. The ribbons show modest macroscopic heterogeneity where, unlike Si-poor Finemets, the surfaces do not squeeze but rather spread the ribbon interior. This effect comes with the optimal percentage of Si also in standard Nb Finemet and the Mo-for-Nb substitution just does not deteriorate the beneficial effect.
- The saturation and the coercivity show the best values for the Mo-only alloy annealed in argon, so there seems to be no need to preserve a tiny percentage of Nb in the composition. Nevertheless, the constricted hysteresis loops observed for vacuum annealed toroids still remain to be clarified.
- The alloy density shows values and annealing behavior not significantly different to standard Nb Finemet. The anisotropic thermal expansion and shrinkage at annealing of as-cast ribbons is observed on Mo Finemets too.
- The Mo-only Finemet responds to annealing under stress along the ribbon axis by significant hard-ribbon-axis magnetic anisotropy, which is fully comparable to an equivalent Nb Finemet.

Acknowledgements

This work was supported in part by the national grant agencies VEGA under Grants no. 2/0156/08, 2/0157/08, 1/0330/09, APVV under Grant no. 0413-06 and Min. Edu of SR under Grant no. AV 4/0025/07. The authors are also grateful to Centrum of Excellence ''Nanosmart'' (SK) and to the bilateral project SAV (SK) – CONICET (RA) for additional support. We also thank prof. M. Liška of Trenčín University for fruitful discussions concerning dilatometry.

References

[1] Y. Yoshizawa, K. Yamauchi, Mater. Sci. Eng. A133 (1991) 176.
[2] M. Müller, N. Mattern, I. Illgen, H.R. Hilzinger, G. Herzer, Key Eng. Mater. 81–83 (1993) 221.
[3] J.S. Blázquez, V. Franco, A. Conde, J. Phys: Condens. Matter 14 (2002) 11717.
[4] M. Pavúk, M. Miglierini, M. Vujtek, M. Mashlan, R. Zboril, Y. Jirásková, J. Phys.: Condens. Matter. 19 (2007) 216219.
[5] V. Franco, C.F. Conde, A. Conde, P. Ochin, J. Non-Cryst. Solids 287 (2001) 366.
[6] J.M. Borrego, C.F. Conde, M. Millán, A. Conde, J.M. Capitán, J.L. Joulaud, Nanostructured Mater. 10 (1998) 575.
[7] L.J. Wang, Y. Pei, L.Y. Wang, Mater. Sci. Eng. A304–306 (2001) 1075.
[8] S. Chikazumi, in: Physics of MagnetismWiley, New York, 1964, p. 17 and 137.
[9] M. Frost, I. Todd, H.A. Davies, M.R.J. Gibbs, R.V. Major, J. Magn. Magn. Mater. 203 (1999) 85.
[10] J.M. Silveyra, E. Illeková, P. Švec, D. Janičkovič, A. Rosales-Rivera, V.J. Cremaschi, Physica B 405 (2010) 2720.
[11] X.Y. Zhang, J.W. Zhang, F.R. Xiao, J.H. Liu, K.Q. Zhang, Y.Z. Zheng, J. Mater. Res. 13 (1997) 3241.
[12] M. Paluga, P. Švec, D. Janičkovič, P. Mrafko, C.F. Conde, J. Non-Cryst. Solids 353 (2007) 2039.
[13] P. Butvin, J. Sitek, B. Butvinová, E. Illeková, J. Phys. IV France 8 (1998) Pr2–123.
[14] P. Butvin, B. Butvinová, J. Sitek, J. Degmová, G. Vlasák, P. Švec, D. Janičkovič, J. Magn. Magn. Mater. 320 (2008) 1133.
[15] J. Lu, J.T. Wang, B.Z. Ding, Scr. Metall. 22 (1988) 1367.
[16] A.L. Mulder, S. van der Zwang, E. Huizer, A. van den Beukel, Scr. Metall. 18 (1984) 515.
[17] P. Butvin, B. Butvinová, G. Vlasák, P. Duhaj, M. Chromčíková, M. Liška, E. Illeková, P. Švec, J. Phys: Conf. Ser. 144 (2009) 012101.
[18] B. Butvinová, G. Vlasák, P. Butvin, E. Illeková, Acta Phys. Slovaca 51 (2001) 1.
[19] S.N. Kane, F. Alves, S.S. Khinchi, A. Gupta, Hyperfine Interact. 183 (2008) 135.
[20] J. Sitek, J. Degmová, P. Butvin, in: Proceedings of the 11th International Workshop APCOM, D. Pudiš, P. Bury, I. Jamnický, I. Martinček (eds.), University of Žilina, SK, 2005, p. 9.
[21] L. Fernández, N. Iturriza, M. Ipatov, J.J. del Val, A. Chizhik, J. González, G. Vara, A.R. Pierna, J. Non-Cryst. Solids 353 (2007) 777.
[22] B. Butvinová, P. Butvin, R. Schäfer, Sensors Actuators A 106 (2003) 52.
[23] S.P. Chenakin, G.G. Galstyan, A.B. Tolstogouzov, N. Kruse, Surf. Interface Anal. 41 (2009) 231.
[24] P. Butvin, B. Butvinová, Z. Frait, J. Sitek, P. Švec, J. Magn. Magn. Mater. 215–216 (2000) 293.
[25] P. Butvin, B. Butvinová, J. Electr. Eng. 50 (1999) 119.